

Multimodal SuperCon: Classifier for Drivers of Deforestation in Indonesia

Bella Septina Ika Hartanti, Valentino Vito, Aniati Murni Arymurthy, Andie Setiyoko

Abstract—Deforestation is one of the contributing factors to climate change. Climate change has a serious impact on human life, and it occurs due to emission of greenhouse gases, such as carbon dioxide, to the atmosphere. It is important to know the causes of deforestation for mitigation efforts, but there is a lack of data-driven research studies to predict these deforestation drivers. In this work, we propose a contrastive learning architecture, called Multimodal SuperCon, for classifying drivers of deforestation in Indonesia using satellite images obtained from Landsat 8. Multimodal SuperCon is an architecture which combines contrastive learning and multimodal fusion to handle the available deforestation dataset. Our proposed model outperforms previous work on driver classification, giving a 7% improvement in accuracy in comparison to a state-of-the-art rotation equivariant model for the same task.

Index Terms—deforestation driver classification, contrastive learning, class imbalance, multimodal fusion

I. INTRODUCTION

Deforestation has become a major problem for the world at large, especially in tropical countries such as Indonesia. Since 2001, the amount of forest area in Indonesia that is overrun by oil palm plantations has doubled, reaching 16.24 Mha in 2019 (64% industrial; 36% smallholder). This amount is more than the official estimates of 14.72 Mha [1]. At the same time, forest area has declined by 11% (9.79 Mha), 32% (3.09 Mha) of which ultimately converted into oil palm plantations, and 29% (2.85 Mha) were both cleared and converted within the same year [1].

Vegetation and soils in forest ecosystems are crucial in regulating various ecosystem processes [2]. Deforestation, both natural or human-made, can cause droughts due to lack of transpiration in the soil. If this disaster continues and becomes large scale, it will have an adverse impact on the climate. To illustrate, the expansion of oil palm plantations in Kalimantan alone is projected to contribute 18–22% of Indonesia’s 2020 carbon emission [3]. Deforestation also has a destructive impact on the ecosystem and biodiversity, and it is becoming a force of global importance [4]. As one of the countries with the most primary forests in the world, Indonesia has a looming threat of major deforestation. Therefore, analyzing and understanding the drivers for deforestation can help to

Bella Septina Ika Hartanti is with the Faculty of Computer Science, Universitas Indonesia, Depok, Indonesia (e-mail: bella.septina@ui.ac.id).

Valentino Vito is with the Faculty of Computer Science, Universitas Indonesia, Depok, Indonesia (e-mail: valentino.vito11@ui.ac.id).

Aniati Murni Arymurthy is with the Faculty of Computer Science, Universitas Indonesia, Depok, Indonesia (e-mail: aniat@cs.ui.ac.id).

Andie Setiyoko is with the Remote Sensing Technology and Data Center, Indonesian National Institute of Aeronautics and Space (LAPAN), Jakarta, Indonesia (e-mail: andie.setiyoko@lapan.go.id).

determine areas in need of reforestation. It also prevents deforestation from becoming more widespread.

Since the advent of high-resolution satellite imaging, disaster analysis typically uses satellite imagery which offers a rich source of information. This can be helpful in determining regions that are currently affected by a disaster, such as deforestation. Prior work have used satellite imagery and deep learning, especially CNN, to solve problems in remote sensing due to their ability to give better performance. In addition, some work have also used multimodal inputs and segmentation to achieve precise predictions of drivers of deforestation in particular. ForestNet [5] implements scene data augmentation and multimodal fusion [6], [7] using CNN models. On top of that, another study [8] introduces the use of rotation-equivariant CNNs on segmentation learning to generate stable segmentation maps with U-Net. However, none of these studies explains in depth the optimal number of auxiliary inputs for the multimodal fusion and the class imbalance naturally present in the dataset.

In this work, we propose a deep learning model, called Multimodal SuperCon, which uses contrastive loss and focal loss for classifying drivers of deforestation in Indonesia. The architecture is chosen due to the class imbalance present in the dataset used in [5]. Using satellite images from Landsat 8, our model consists of two stages of training, namely representation training as the first stage and classifier fine-tuning as the second stage. Our model is a modification of an established architecture known as SuperCon [9], and it allows multimodal fusion in the classifier fine-tuning stage.

II. RELATED WORK

A. Machine Learning for Deforestation Analysis

To our knowledge, there have been two proposed deep learning models for handling the deforestation driver classification task in Indonesian forest regions. The first was the ForestNet architecture introduced by Irvin *et al.* [5] in 2020, and the second was a rotation equivariant CNN architecture applied by Mitton and Murray-Smith [8] in 2021.

ForestNet [5] is a semantic segmentation architecture that is created to (1) address that there are often multiple land uses within a single forest loss image, and (2) implicitly utilize the information of specific loss regions. ForestNet allows for predictions from high-resolution (15m) images to predict different drivers of multiple loss regions with varying sizes. The model also incorporates a type of data agumentation named scene data augmentation (SDA), per-pixel classification, and multimodal fusion in its architecture.

Many research studies in deep learning use convolutional neural networks (CNN) due to their powerful capabilities to process sensory data such as images and videos. A CNN model consists of multiple convolutional layers which are translation equivariant. In other words, if an input image is translated to any direction, the result of the feature map is shifted accordingly. However, standard convolutional layers are not rotation equivariant, which can be crucial in order to ensure that the model performs well in certain applications. To make the convolutional layers rotation equivariant, architectures involving group equivariant CNNs can be employed [10], [11], [12]. Rotation equivariant CNNs built using this method has been successfully applied in [8] to the same deforestation dataset used by Irvin *et al.* [5].

B. Contrastive Learning

Contrastive learning is a representation learning approach that aims to shape the feature space in such a way that similar (or positive) samples are clustered together, while dissimilar (or negative) samples are pushed apart. In the past, contrastive learning is executed in a self-supervised manner, with every anchor having exactly one positive sample [13], [14], [15], [16]. This positive sample can be obtained by, for example, applying data augmentation to the anchor.

Khosla *et al.* [17] introduced the concept of supervised contrastive learning, which allows an anchor to have multiple positive samples. The positive samples of an anchor consists of samples that belong to the same class as the anchor. In effect, supervised contrastive learning aims to minimize the distance of intra-class samples and maximize the distance of inter-class samples in the feature space. In practice, supervised contrastive learning is done using the contrastive loss, whose formula is shown in Eq. (1).

C. Class Imbalance in Datasets

Class imbalance occurs when the majority of data in a dataset is classified as a certain class. This imbalance may cause difficulty in training the model using data from the minority classes. Several methods have been proposed in the past to deal with class imbalance. One popular solution is by either undersampling the majority class [18], [19] or oversampling the minority class [20], [21] so that the dataset becomes balanced.

Another way to ensure that the model learns from the minority classes is by modifying the loss function. Despite being the most popular classification loss, the cross-entropy loss is often not the most suitable choice for handling imbalanced datasets. Focal loss [22], [23], shown in Eq. (3), is a widely used modification of cross-entropy loss that is able to focus on hard-to-classify samples. Consequently, focal loss is a more suitable option when dealing with class imbalance. Another loss function that has been successfully utilized is the contrastive loss. A training strategy involving contrastive learning has been shown to be more effective or at least on par compared to cross-entropy and focal loss [24], [9].

III. METHODOLOGY

The model that we apply to the deforestation dataset is built upon the SuperCon architecture [9]. SuperCon is a two-stage, contrastive learning architecture consisting of a representation training stage and a classifier fine-tuning stage. The resulting model is used for handling classification tasks. During the representation training stage, the ResNet encoder backbone learns from data using the contrastive loss. Afterwards, the classifier fine-tuning stage is used to train a classification layer which generates an estimated probability for each class label. SuperCon works well on datasets under settings involving class imbalance [9].

We propose Multimodal SuperCon, a modification of SuperCon with the addition of multimodal fusion during classifier fine-tuning. This way, the model can learn from a variety of data in order to obtain a more accurate result. In our application to the deforestation dataset, Multimodal SuperCon allows the use of auxiliary predictors, such as slope, aspect, and elevation, in addition to the satellite images. The architecture of Multimodal SuperCon is illustrated in Fig. 1. The following subsections explain the two stages of Multimodal SuperCon in more detail.

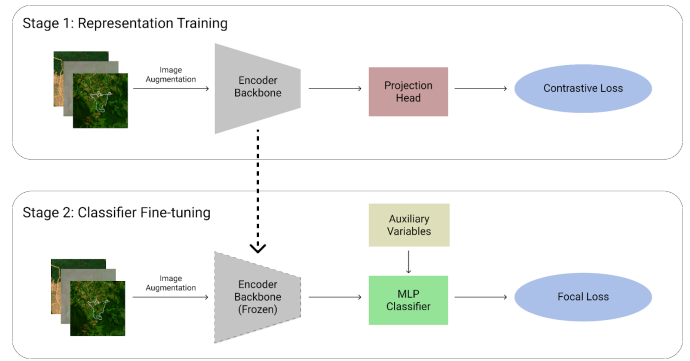


Fig. 1. The Architecture of Multimodal SuperCon

A. Representation Training

Let $\{\mathbf{x}_1, \dots, \mathbf{x}_N\}$ be a mini-batch of augmented training samples from the dataset with batch size N . The features of each training sample \mathbf{x}_i are extracted using the encoder backbone Enc_θ . In practice, the encoder uses a pre-trained model, such as the ResNet or UNet architecture. The encoder Enc_θ generates a representation $\text{rep}_i = \text{Enc}_\theta(\mathbf{x}_i)$, which is then projected using the projection head Proj .

The projection head is a two-layer network of size 2048 and 128, respectively. It generates a lower-dimensional representation $\mathbf{z}_i = \text{Proj}(\text{rep}_i)$ of each training sample \mathbf{x}_i . Each \mathbf{z}_i is L_2 -normalized ($\|\mathbf{z}_i\|_2 = 1$) so that \mathbf{z}_i lies on the unit hypersphere. Afterwards, contrastive loss is applied to the set $\{\mathbf{z}_1, \dots, \mathbf{z}_N\}$:

$$\mathcal{L}_{\text{con}} = - \sum_{i=1}^n \frac{1}{|P_i|} \sum_{\mathbf{z}_j \in P_i} \log \left(\frac{\exp(\mathbf{z}_i \cdot \mathbf{z}_j / \tau)}{\sum_{\mathbf{z}_k \in A_i} \exp(\mathbf{z}_i \cdot \mathbf{z}_k / \tau)} \right) \quad (1)$$

The notation P_i denotes the set of positive samples of the anchor \mathbf{z}_i (that is, samples \mathbf{z}_j in the mini-batch other than

z_i having the same class label as z_i). On the other hand, A_i denotes the set of samples z_k in the mini-batch other than z_i .

Contrastive loss serves to contrast the training samples among themselves in order to shape the feature space according to class labels. The loss contains the temperature parameter τ . The parameters θ of the encoder Enc_θ are then updated according to the gradient of the contrastive loss:

$$\theta_{n+1} \leftarrow \theta_n - \lambda \cdot \nabla \mathcal{L}_{\text{con}}, \quad (2)$$

where n is the iteration index and λ is the learning rate.

B. Classifier Fine-Tuning

In the fine-tuning stage, the encoder backbone is frozen so that training is focused on the classifier Clas_φ . Each training sample x_i is fed through the trained encoder to generate $\text{rep}_i = \text{Enc}_\theta(x_i)$. Afterwards, rep_i is concatenated with the extracted features aux_i of the auxiliary variables to generate $\text{rep}'_i = \text{rep}_i \parallel \text{aux}_i$. This concatenation is the process in which multimodal fusion occurs.

The MLP classifier Clas_φ takes rep'_i as input to generate an estimated probability for every class. Unlike regular SuperCon, Clas_φ consists of multiple layers instead of just one in order to handle the multimodal fusion. Let p_t be the estimated probability of the ground-truth class label of x_i . The classification loss of the model is calculated using the focal loss:

$$\mathcal{L}_{\text{foc}} = -\alpha_t (1 - p_t)^\gamma \log(p_t) \quad (3)$$

The loss $\mathcal{L}_{\text{CE}} = \log(p_t)$ is simply the standard cross-entropy loss. Therefore, focal loss is a generalization of cross-entropy loss.

Focal loss contains two parameters: the balancing parameter α_t of the ground truth label and the focusing parameter γ . Since the encoder is frozen, only the parameters φ of the classifier Clas_φ are updated according to the gradient of the focal loss:

$$\varphi_{n+1} \leftarrow \varphi_n - \lambda \cdot \nabla \mathcal{L}_{\text{foc}}, \quad (4)$$

where n is the iteration index and λ is the learning rate.

IV. EXPERIMENTS

A. Experimental Datasets

We use the public Landsat8 image dataset on deforestation in Indonesia to train and test our model. This dataset is the same as the dataset used in [5], [8]. The driver annotations and coordinates for forest loss events were curated by Austin *et al.* [25]. The dataset consists of 1616 data for training, 473 data for validation, and 668 data for testing. The forest loss images were obtained from various regions no more than five years after deforestation occurred in the area. Each image is classified into one of four classes: grassland/shrubland, plantation, smallholder agriculture, or other. The classes represent the drivers of deforestation of the forest loss region shown in a satellite image. As shown in Fig. 2, the data distribution for the four classes is imbalanced, with most of the data belonging to the plantation class.

The original dataset is collected from forest loss events at 30m resolution from 2001 to 2016 in various Indonesian

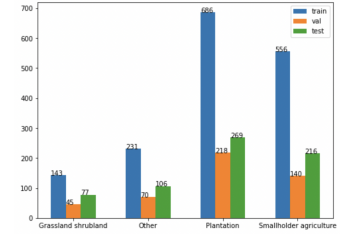


Fig. 2. The Distribution of The ForestNet Dataset by Class

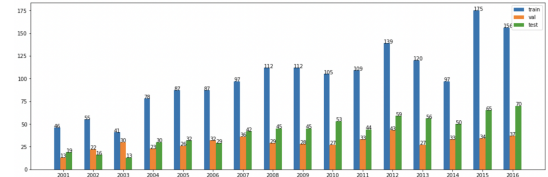


Fig. 3. The Distribution of The ForestNet Dataset Based on Year of Occurrence of The Forest Loss Event

islands. Fig. 3 shows the distribution of data based on when the forest loss event occurred. Due to the lack of availability of Landsat 8 imagery, which is used for constructing composite images as input data, we only use data obtained in the last five years. Each forest loss region is represented as a polygon, indicating the forest loss event within a year. On the other hand, the composite images are represented as an RGB image with a total size of 332 x 332 pixels to capture the forest loss. We also use auxiliary predictors in addition to the images so that we are able to employ multimodal fusion to the classification task. The auxiliary predictors used in our experiment are slope, altitude, aspect, and gain. Fig. 4 provides an example of the data used in this research.

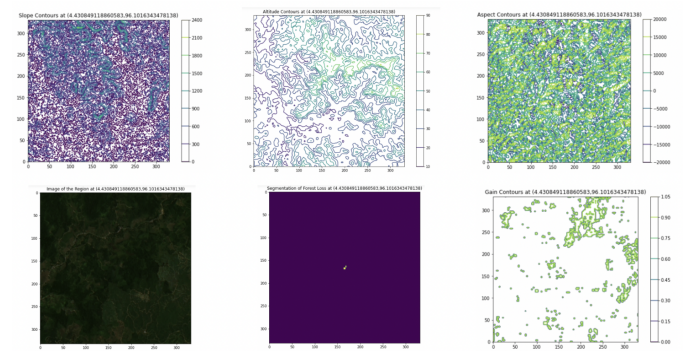


Fig. 4. An Illustration of a Landsat 8 Imaging Datum Along With Contour Plots of Its Auxiliary Variables

B. Experimental Settings

We use the PyTorch framework to build our Multimodal SuperCon model¹. We implement several data augmentation techniques, including horizontal flip, rotation, and elastic transform, in order to increase the robustness of the model. The model is trained on NVIDIA DGX A100 with 64 GB

¹Source code: https://github.com/bellasih/multimodal_supercon

memory for roughly 45 minutes. In addition, we use the Adam optimizer and a learning rate of $\lambda = 10^{-3}$ during training. We set aside 15 epochs for the representation training of the encoder backbone and 10 epochs for the classifier fine-tuning. The batch size for both stages is set to 16.

We use EfficientNet-B2 [26] as the encoder backbone for the Multimodal Supercon architecture. For comparison purposes, we also utilize the ResNet18 [27] and UNet [28] pre-trained models as substitute encoders. We set $\tau = 0.1$ for the contrastive loss, and $\alpha = 0.8$ and $\gamma = 2$ for the focal loss. The architecture is trained a total of three times using only one auxiliary variable (slope), two auxiliary variables (slope and altitude), and all four auxiliary variables (slope, altitude, aspect, and gain), respectively. We compare the performance of our model to the CNN models used in [8] as baselines.

C. Results and Discussion

From Tables I and II, the experimental results show that the proposed model (Multimodal SuperCon using EfficientNet-B2 as the encoder and MLP as the classifier) gave the best performance. Compared to other models (ResNet18 as the encoder with MLP; Vanilla U-Net as the encoder with MLP), EfficientNet-B2 excels both during the representation training stage and the classifier fine-tuning stage. The proposed model gave an accuracy of 66% when using one auxiliary variable (slope) and two auxiliary variables (slope and altitude). An accuracy of 70% is obtained when using all four auxiliary variables during classifier training. Also, the proposed model gave lower loss on representation learning, namely 0.49 using one auxiliary variable, 0.52 using two auxiliary variables, and 0.48 using four auxiliary variables. These differences indicate that the use of an appropriate pre-trained model is crucial to obtain better performance. EfficientNet outperforms not only in terms of accuracy and loss, but also in terms of computation time.

On the optimal number of auxiliary variables used, the best model gave an accuracy of 70% and a loss of 0.48 when using all four auxiliary variables. This indicates that the addition of several relevant inputs can give more information to the model, hence benefiting training. From Table III, our proposed model also outperforms the results of the baseline model for the same task, namely the rotation equivariant CNN architecture, which yields an accuracy of only 63% [8].

TABLE I
THE PERFORMANCE OF MULTIMODAL SUPERCON ON REPRESENTATION LEARNING

	Evaluation (Loss)		
	1 Aux	2 Aux	4 Aux
ResNet18 + MLP	0.56	0.57	0.59
EfficientNet + MLP	0.49	0.52	0.48
UNet + MLP	0.56	0.56	0.56

V. CONCLUSION AND FUTURE WORK

In this paper, we introduced Multimodal SuperCon, a two-stage training architecture involving multimodal fusion to

TABLE II
THE PERFORMANCE OF MULTIMODAL SUPERCON ON CLASSIFIER LEARNING

	Evaluation (Accuracy)		
	1 Aux	2 Aux	4 Aux
ResNet18 + MLP	0.47	0.55	0.51
EfficientNet + MLP	0.66	0.66	0.70
UNet + MLP	0.55	0.54	0.59

TABLE III
A COMPARISON BETWEEN THE PERFORMANCE OF MULTIMODAL SUPERCON AND BASELINE CNN MODELS

	Test accuracy
UNet - CNN [8]	0.58
UNet - C8 Equivariant [8]	0.63
Multimodal SuperCon (1 Aux)	0.66
Multimodal SuperCon (2 Aux)	0.66
Multimodal SuperCon (4 Aux)	0.70

handle the class imbalance present within the deforestation dataset used in [5], [8]. We applied Multimodal SuperCon to the public Landsat8 imaging dataset consisting of data on forest loss regions in Indonesia. The EfficientNet-B2 + MLP model gave superior performance compared to other encoder architectures, and the resulting test accuracy was significantly higher than the accuracy obtained by the CNN models in [8]. It was also shown that multimodal fusion is essential in order to yield good results. By using all four auxiliary predictors, the model was able to perform better with an accuracy of 70%.

In the future, Multimodal SuperCon can be applied to a dataset not necessarily on deforestation datasets, but on any domain requiring some form of multimodal fusion. The model can also be modified for other uses both in deep learning and remote sensing. EfficientNet should be a strong candidate for the encoder backbone since it performs significantly better than other pre-trained models including ResNet18 and UNet.

VI. ACKNOWLEDGMENT

We thank the support of Tokopedia-UAI Center of Excellence, Faculty of Computer Science, University of Indonesia, for providing access to the NVIDIA DGX-A100 to run the experiments.

REFERENCES

- [1] David L. A. Gaveau, Bruno Locatelli, Mohammad A. Salim, Husnayaen, Timer Manurung, Adrià Descals, Arild Angelsen, Erik Meijaard, and Douglas Sheil. Slowing deforestation in indonesia follows declining oil palm expansion and lower oil prices. *PLOS ONE*, e0266178, 2022.
- [2] Almut Arneth, Fatima Denton, Fahmuddin Agus, Aziz Elbehri, Karl Heinz Erb, B Osman Elasha, Mohammad Rahimi, Mark Rounsevell, Adrian Spence, Riccardo Valentini, et al. Framing and context. In *Climate Change and Land: an IPCC special report on climate change, desertification, land degradation, sustainable land management, food security, and greenhouse gas fluxes in terrestrial ecosystems*, pages 1–98. Intergovernmental Panel on Climate Change (IPCC), 2019.
- [3] Kimberly M Carlson, Lisa M Curran, Gregory P Asner, Alice McDonald Pittman, Simon N Trigg, and J Marion Adeney. Carbon emissions from forest conversion by kalimantan oil palm plantations. *Nature Climate Change*, 3(3):283–287, 2013.

- [4] Jonathan Foley, Ruth Defries, Gregory Asner, Carol Barford, Gordon Bonan, Stephen Carpenter, F Stuart Chapin III, Michael Coe, Gretchen Daily, Holly Gibbs, Joseph Helkowski, Tracey Holloway, Erica Howard, Christopher Kucharik, Chad Monfreda, Jonathan Patz, Iain Prentice, Navin Ramankutty, and Peter Snyder. Global consequences of land use. *Science (New York, N.Y.)*, 309:570–4, 08 2005.
- [5] Jeremy Irvin, Hao Sheng, Neel Ramachandran, Sonja Johnson-Yu, Sharon Zhou, Kyle Story, Rose Rustowicz, Cooper Elsworth, Kemen Austin, and Andrew Y. Ng. Forestnet: Classifying drivers of deforestation in indonesia using deep learning on satellite imagery. *CoRR*, abs/2011.05479, 2020.
- [6] Pradeep K Atrey, M Anwar Hossain, Abdulmotaleb El Saddik, and Mohan S Kankanhalli. Multimodal fusion for multimedia analysis: a survey. *Multimedia systems*, 16(6):345–379, 2010.
- [7] Hao Sheng, Xiao Chen, Jingyi Su, Ram Rajagopal, and Andrew Ng. Effective data fusion with generalized vegetation index: Evidence from land cover segmentation in agriculture. In *Proceedings of the IEEE/CVF Conference on Computer Vision and Pattern Recognition Workshops*, pages 60–61, 2020.
- [8] Joshua Mitton and Roderick Murray-Smith. Rotation equivariant deforestation segmentation and driver classification. *CoRR*, abs/2110.13097, 2021.
- [9] Keyu Chen, Di Zhuang, and J. Morris Chang. SuperCon: Supervised contrastive learning for imbalanced skin lesion classification, 2022.
- [10] Maurice Weiler and Gabriele Cesa. General E(2)-equivariant steerable CNNs. *CoRR*, abs/1911.08251, 2019.
- [11] Taco Cohen and Max Welling. Group equivariant convolutional networks. In *International conference on machine learning*, pages 2990–2999. PMLR, 2016.
- [12] Taco S Cohen and Max Welling. Steerable CNNs. *arXiv preprint arXiv:1612.08498*, 2016.
- [13] Ting Chen, Simon Kornblith, Mohammad Norouzi, and Geoffrey Hinton. A simple framework for contrastive learning of visual representations. In *International conference on machine learning*, pages 1597–1607. PMLR, 2020.
- [14] Olivier Henaff. Data-efficient image recognition with contrastive predictive coding. In *International Conference on Machine Learning*, pages 4182–4192. PMLR, 2020.
- [15] R Devon Hjelm, Alex Fedorov, Samuel Lavoie-Marchildon, Karan Grewal, Phil Bachman, Adam Trischler, and Yoshua Bengio. Learning deep representations by mutual information estimation and maximization. *arXiv preprint arXiv:1808.06670*, 2018.
- [25] Kemen G Austin, Amanda Schwantes, Yaofeng Gu, and Prasad S Kasibhatla. What causes deforestation in indonesia? *Environmental Research Letters*, 14(2):024007, 2019.
- [16] Yonglong Tian, Dilip Krishnan, and Phillip Isola. Contrastive multiview coding. In *European conference on computer vision*, pages 776–794. Springer, 2020.
- [17] Prannay Khosla, Piotr Teterwak, Chen Wang, Aaron Sarna, Yonglong Tian, Phillip Isola, Aaron Maschinot, Ce Liu, and Dilip Krishnan. Supervised contrastive learning. *CoRR*, abs/2004.11362, 2020.
- [18] Chris Drummond, Robert C Holte, et al. C4. 5, class imbalance, and cost sensitivity: why under-sampling beats over-sampling. In *Workshop on learning from imbalanced datasets II*, volume 11, pages 1–8. Citeseer, 2003.
- [19] Haibo He and Edwardo A Garcia. Learning from imbalanced data. *IEEE Transactions on knowledge and data engineering*, 21(9):1263–1284, 2009.
- [20] Junran Peng, Xingyuan Bu, Ming Sun, Zhaoxiang Zhang, Tieniu Tan, and Junjie Yan. Large-scale object detection in the wild from imbalanced multi-labels. In *Proceedings of the IEEE/CVF Conference on Computer Vision and Pattern Recognition*, pages 9709–9718, 2020.
- [21] Li Shen, Zhouchen Lin, and Qingming Huang. Relay backpropagation for effective learning of deep convolutional neural networks. In *European conference on computer vision*, pages 467–482. Springer, 2016.
- [22] Tsung-Yi Lin, Priya Goyal, Ross B. Girshick, Kaiming He, and Piotr Dollár. Focal loss for dense object detection. *CoRR*, abs/1708.02002, 2017.
- [23] Michael Yeung, Evis Sala, Carola-Bibiane Schönlieb, and Leonardo Rundo. Unified focal loss: Generalising dice and cross entropy-based losses to handle class imbalanced medical image segmentation. *Computerized Medical Imaging and Graphics*, 95:102026, 2022.
- [24] Yassine Marrakchi, Osama Makansi, and Thomas Brox. Fighting class imbalance with contrastive learning. In *International Conference on Medical Image Computing and Computer-Assisted Intervention*, pages 466–476. Springer, 2021.
- [26] Mingxing Tan and Quoc Le. Efficientnet: Rethinking model scaling for convolutional neural networks. In *International conference on machine learning*, pages 6105–6114. PMLR, 2019.
- [27] Kaiming He, Xiangyu Zhang, Shaoqing Ren, and Jian Sun. Deep residual learning for image recognition. In *Proceedings of the IEEE conference on computer vision and pattern recognition*, pages 770–778, 2016.
- [28] Olaf Ronneberger, Philipp Fischer, and Thomas Brox. U-net: Convolutional networks for biomedical image segmentation. In *International Conference on Medical image computing and computer-assisted intervention*, pages 234–241. Springer, 2015.